Title

3D surface topology guides stem cell adhesion and differentiation

Journal

Biomaterials, 52(1)

ISSN

0142-9612

Authors

Viswanathan, Priyalakshmi

Ondeck, Matthew G

Chirasatitsin, Somyot

et al.

Publication Date

2015-06-01

DOI

10.1016/j.biomaterials.2015.01.034

Peer reviewed

Biomaterials 52 (2015) 140–147

Contents lists available at ScienceDirect

Biomaterials

journal homepage: www.elsevier.com/locate/biomaterials

3D surface topology guides stem cell adhesion and differentiation

Priyalakshmi Viswanathan [a, b, 2], Matthew G. Ondeck [c, d, 2], Somyot Chirasatitsin [e, 1], Kamolchanok Ngamkham [f, g], Gwendolen C. Reilly [h], Adam J. Engler [c, d, e, *], Giuseppe Battaglia [f, g, **]

[a] Krebs Institute, The University of Sheffield, Sheffield S10 2TN, UK
[b] Department of Biomedical Sciences, The University of Sheffield, Sheffield S10 2TN, UK
[c] Sanford Consortium for Regenerative Medicine, University of California, San Diego, La Jolla, CA 92037, USA
[d] Material Science Program, University of California, San Diego, La Jolla, CA 92093, USA
[e] Department of Bioengineering, University of California, San Diego, La Jolla, CA 92093, USA
[f] Department of Chemistry, University College London, London WC1H 0AJ, UK
[g] The MRC/UCL Centre for Medical Molecular Virology, University College London, London WC1H 0AJ, UK
[h] Department of Materials Science and Engineering, Insigneo Institute for in silico Medicine, The University of Sheffield, Sheffield S1 3JD, UK

ARTICLE INFO

Article history:
Received 24 September 2014
Received in revised form
30 December 2014
Accepted 20 January 2015
Available online

Keywords:
Surface topology
Osteogenesis
Stem cell
Cell signaling

ABSTRACT

Polymerized high internal phase emulsion (polyHIPE) foams are extremely versatile materials for investigating cell–substrate interactions *in vitro*. Foam morphologies can be controlled by polymerization conditions to result in either open or closed pore structures with different levels of connectivity, consequently enabling the comparison between 2D and 3D matrices using the same substrate with identical surface chemistry conditions. Additionally, here we achieve the control of pore surface topology (i.e. how different ligands are clustered together) using amphiphilic block copolymers as emulsion stabilizers. We demonstrate that adhesion of human mesenchymal progenitor (hES-MP) cells cultured on polyHIPE foams is dependent on foam surface topology and chemistry but is independent of porosity and interconnectivity. We also demonstrate that the interconnectivity, architecture and surface topology of the foams has an effect on the osteogenic differentiation potential of hES-MP cells. Together these data demonstrate that the adhesive heterogeneity of a 3D scaffold could regulate not only mesenchymal stem cell attachment but also cell behavior in the absence of soluble growth factors.

1. Introduction

Cell interactions with their surrounding extracellular matrix (ECM) play an important role in regulating cellular functions as basic as proliferation [1,2] and as complex as stem cell differentiation [3–5]. It has become widely appreciated that the properties of this cell-ECM interface, including surface topography [6,7], hydrophobicity and hydrophilicity [8], and surface chemistry [4,7,9], must mimic those of native ECM to appropriately guide cell function. Spatial and temporal patterns of these cues are equally important in regulating function [10]. More importantly, the configuration of these physical cues, i.e. their topology, is critical in controlling cellular function by matching the endogenous topology of the cell membrane to enhance signaling and function. One way to understand this is the design of surfaces where chemistries are arranged in different patterns that create different topological cues to control cell adhesion and hence signaling. Previous studies have showed that patterns of click chemistry [11], photolithography (by UV crosslinking) [11-13], and alkanethiol self-assembled monolayers (SAMs) [14,15] all directed cell adhesion and lineage specification. For example, adhesive sites spaced 34 or 62 nm apart directed mesenchymal stem cells (MSCs) to mature into osteoblasts or adipose cells, respectively [16]. Yet ECM proteins such as fibronectin exhibit heterogeneously distributed cell binding sites [17]

* Corresponding author. Department of Bioengineering, University of California, San Diego, La Jolla, CA 92093, USA.
** Corresponding author. Department of Chemistry and University College London, London WC1H 0AJ, UK.
E-mail addresses: aengler@ucsd.edu (A.J. Engler), g.battaglia@ucl.ac.uk (G. Battaglia).
[1] Present address: Department of Biomedical Engineering, Prince of Songlkla University, Hat Yai, Thailand.
[2] Equal contribution.

http://dx.doi.org/10.1016/j.biomaterials.2015.01.034
0142-9612/

that are exquisitely controlled at the nanometer length scale [18]. When ligand spacing is similarly disordered [19] with spacing >70 nm, stem cell adhesion and function improve [20]. However, ECM is a 3D network and these patterning methods are limited to planar substrates.

To overcome this challenge, high internal phase emulsion (HIPE) templated matrices have been used to different topological arrangements of ligand spacing in 3D foams [21,22]. The water-in-oil HIPE matrix can be stabilized by two amphiphilic block co-polymers: poly(1,4-butadiene)-b-poly(ethylene glycol) (PBD-PEO) and polystyrene-b-poly(acrylic acid) (PS-PAA) [21]. By using co-polymers with dissimilar hydrophilic blocks, their phase separation at the oil-water interface could be exploited upon polymerization of the HIPE template [23,24], resulting in foams surface functionalized *in situ* with domains of either PEO or PAA. This created topologically defined 3D foams with domains that were cell inert (PEO) or charged to facilitate protein deposition and thus cell adhesion (PAA). Adhesive domain areas ranged from tens to hundreds of square nanometers creating unique "surface topology." We previously determined that foams exhibiting smaller adhesive domains that were spaced hundreds of nanometers apart supported the most robust human mesenchymal progenitor (hES-MP) adhesion [21]. One drawback of these PAA/PEO foams was that they lacked appreciable interconnectivity that limits cell infiltration unlike the open lattice found in native ECM [17]. Consequently here, we synthesized foams with closed as well as open pore structures [25,26] to determine if scaffold morphology and pore interconnectivity regulated stem cell adhesion and differentiation.

2. Materials and methods

2.1. Scaffold preparation

All chemicals were purchased from Sigma Aldrich unless otherwise stated. Styrene and divinylbenzene (80% technical grade) monomers were passed through a column of activated basic alumina (Brockmann Activity I) to remove the inhibitor p-tert butylcatechol prior to use. The initiators $K_2S_2O_8$ and azobisisobutyronitrile (AIBN; Fisher Scientific), tetrahydrofuran, block copolymers poly(1,4-butadiene)-b-poly(ethylene oxide) (PBD-PEO, Mw = 14,700 g/M) and polystyrene-b-poly(acrylic acid) (PS-PAA, Mw = 18,600) (PolymerSource Inc., Montreal), and the surfactant Span 80 were all used as received and all copolymers have a reported polydispersity index (PDI) of 1.1–1.3.

High internal phase emulsions were prepared in a method adapted from Viswanathan and coworkers [21]. Briefly, the surfactant was solubilized in the oil phase at 0.01 mol% (relative to the monomer) in all cases. For copolymers mixtures of PBD-PEO and PS-PAA, the surfactants were used in molar ratios 75:25, 50:50, and 25:75 as defined in Table 1. Resulting foams are herein referred to by their PEO molar content, e.g. 25% PEO will be PEO25, except for pure PS-PAA, which will be referred to as PAA100. THF (10 μL/mg) was used to dissolve PS-PAA before its addition to the oil phase due to its poor solubility in styrene/divinylbenzene (Sty/DVB). The aqueous phase was added using a peristaltic pump at a rate of 10 ml/min, which was continuously stirred at 750 rpm. All emulsions had an aqueous phase volume fraction of 90%. For closed porous foams, the aqueous phase contained 0.1 w/v % radical initiator $K_2S_2O_8$. For open porous foams, the oil phase contained 1 w/w % radical initiator AIBN, which was added immediately prior to emulsification. The resulting emulsions were polymerized at 50 °C for 24 h, Soxhlet extracted in isopropyl alcohol for 24 h to remove unreacted monomers, and vacuum dried prior to use. Emulsions were stabilized with the surfactant Span 80 and were prepared using previously established protocols [27] as a control for the 3D foam architecture.

Table 1
Foam compositions based on their mixture of PBD and PAA as well as the nomenclature used in the study.

Foam nomenclature	PBD-PEO mole fraction	PS-PAA mole fraction
PEO100	100	0
PEO75	75	25
PEO50	50	50
PEO25	25	75
PAA100	0	100

2.2. 3D cell culture

Human Embryonic Stem cell derived Mesenchymal Progenitor cells (hES-MP™, Cellectis, UK), which differentiate towards osteogenic, chondrogenic and adipogenic lineages [28], were used in all experiments. We have previously shown hES-MPs to express the bone markers alkaline phosphatase and mineralized matrix [29]. Cells were cultured in growth media containing Alpha modified Minimum Essential Medium (Alpha-MEM, Gibco, UK) supplemented with 10% fetal bovine serum (FBS), 1% Penicillin/Streptomycin (Invitrogen, UK) and 10 ng/ml basic-fibroblast growth factor (b-FGF, Invitrogen, UK). Cells were maintained in a humidified 37 °C incubator at 5% CO_2. Cultures were passaged at 70–80% confluence using Trypsin EDTA and used at passages between 5 and 10.

Scaffolds (1.2 cm in diameter and 3–5 mm in high) were sterilized for cell culture using 70% ethanol (EtOH) overnight and then washed three times with PBS to remove EtOH. To prevent scaffold buoyancy in the well plate, they were weighed down with custom dental grade stainless steel rings for the first week in culture. Scaffolds were washed once with media before seeding with hES-MP cells at a density of 100,000 cells/scaffold in 50 μL media. Cells were incubated at 37 °C for 90 min before adding 1 ml of media/well without b-FGF. After 24 h of seeding, scaffolds were transferred to a new well plate with subsequent media changes every 2–3 days. For experiments investigating mineral deposition, hES-MPs seeded on scaffolds were treated with 10 nM dexamethasone (Dex) 24 h after seeding. Cells used in the MTT, Alamar Blue, and Titertacs Apoptosis assays (all from Invitrogen) were all cultured for 7 days on the indicated substrates prior to use in the assay, which were performed according to manufacturer instructions with positive and negative controls on tissue culture plastic.

2.3. Cell morphology by confocal microscopy

Cells were fixed and stained for nuclear and actin staining on days 7, 14, 21 and 28 as follows. Scaffolds were washed once with PBS and fixed with 3.7% formaldehyde for 40 min then permeabilized with 0.1% Triton X for 20 min. Cells were then incubated with Phalloidin-Texas Red (1:100 in PBS) and DAPI (25 μL) for 1 h on a plate rocker at room temperature. Unbound stain was washed with PBS three times and scaffolds were stored in PBS at 4 °C until imaged. Imaging was performed using an inverted Zeiss LSM 510 confocal laser scanning microscope with a 10× objective.

2.4. SEM imaging

Sectioned foams were prepared for scanning electron microscopy (SEM) by placing each foam on an aluminum stub with an adhesive carbon pad. Samples were coated with 15 nm gold (Edwards S150B Sputter Coater) prior to SEM using a Philips XL20 scanning electron microscope at an accelerating voltage of 10 kV and spot size of 3.0 nm. Scaffold void and interconnect diameters were measured from scanning electron micrographs using Image J.

For biological SEM, cells cultured on foams for 28 days were fixed in 2.5% glutaraldehyde (1 mL/well) overnight. Scaffolds were then rinsed in PBS twice for 15 min each followed by dH_2O once for 15 min. Samples were then dehydrated using an EtOH gradient of 35%, 60%, 80%, 90% and absolute EtOH for 15 min each. Scaffolds were then critically dried using a 1:1 v:v of absolute EtOH:hexamethyldisilazane for 1 h. This was followed by a hexamethyldisilazane wash twice, each for 10 min before samples were left to dry completely under vacuum. Samples were then sputter coated and viewed under SEM as previously described.

2.5. Calcium staining by alizarin red S

hES-MP cells cultured on open porous scaffolds for 28 days were fixed in 3.7% formaldehyde for 30 min and washed with PBS once and in dH_2O twice. Alizarin Red S (0.5 w/v%) in dH_2O was adjusted to a pH of 4.1 using 0.1 M NaOH. 1 ml was added to each scaffold and placed on a rocker for 30 min. Scaffolds were then washed three times in dH_2O to remove unbound stain and left to air dry. Blank scaffolds were also treated with Alizarin Red to assess baseline staining. To quantify mineral deposition, 0.5 ml of perchloric acid (5% v/v% in dH_2O) was added to each scaffold to de-stain it. 200 μL of the de-staining solution was pipetted to a 96 well plate and absorbance read at 405 nm.

2.6. RNA isolation, cDNA synthesis, and qPCR microarrays

hES-MP cells were cultured on both closed and open porous foams for 7 days. Scaffolds were washed once with PBS and total RNA was extracted using the Qiagen RNAse Mini Kit (Qiagen, UK). Reverse transcription was performed using 5 μg total RNA to obtain cDNA using the QuantiTect Reverse Transcription Kit (Qiagen, UK). Genomic DNA was eliminated from RNA samples by incubating samples with Wipeout buffer for 2 min at 42 °C prior to reverse transcription. Resulting cDNA samples were then placed in a customized 384 well Taqman microarray (Applied Biosystems; for genes, see Supplemental Table 1) to detect gene expression. The array plate was analyzed by RT-PCR using the 7900HT RT-PCR system (Applied Biosystems). The reactions were amplified for 40 cycles. Ct values were acquired from amplification curves in triplicate, and relative fold change was computed using the ΔΔCt method [30]. Gene expression was expressed as a fold change of the cells cultured in each foam composition versus cells maintained on tissue culture

plastic plates in standard media (without supplements intended to induce differentiation).

2.7. Statistical analysis

All experiments were performed in triplicate for three samples per condition (n=9) unless otherwise noted. All values reported are average ± standard deviation unless otherwise noted. One-way ANOVA with appropriate Tukey post-hoc analysis was performed to test for significance between two sample means unless otherwise noted.

3. Results

Block copolymer functionalized polyHIPE foams were synthesized to generate either closed or open pore morphologies by the addition of either a water or oil soluble radical initiator, i.e. $K_2S_2O_8$ or AIBN, to created closed (Fig. 1A) or interconnected pores (Fig. 1B), respectively. Herein, open porous refers to foams with an interconnected 3D structure while closed porous refers to foams with a lack of interconnectivity between adjacent pores. Open porous foams functionalized with either PEO, PAA, or their mixtures exhibited pore sizes in the range of 40–80 μm (Supplemental Figure 1A and green arrow). Additionally, average interconnected pore diameters did not exhibit statistically significant changes with surface chemistry (Supplemental Figure 1B and red arrow). Relative to closed porous foams [21], average pore size diameters did not differ significantly. Roughness of the open porous foam surfaces also appeared lower and uniform relative to closed porous foams based on SEM images (Fig. 1). Thus, pore size and the level of interconnectivity within each foam type was independent of surface chemistry and pore size was independent of initiator.

Given previous segregation of copolymer mixtures in closed porous foams, we next investigated how similar segregation of the same copolymers in open porous foams, shown schematically in Fig. 2 as 'topology,' could affect adhesion. Human embryonic stem cell derived mesenchymal progenitor cells (hES-MP) were cultured for a period of 7 days in the absence of any specific growth factors. Cell viability was first assessed by MTT and alamar blue assays to determine cell viability (metabolic activity) and relative cell number as a function of copolymer composition and pore morphology. While MTT showed higher cell viability on open versus closed pore foams, mixed copolymer compositions, which had previously been identified to have adhesive nano-domains, e.g. PEO50 and PEO75 [21], retained the most cells independent of pore morphology (Supplemental Figure 2A). Alamar blue staining also confirmed higher cell viability on mixed versus single copolymer compositions for open pore foams (Supplemental Figure 2B); little apoptosis was detected for open pore foams and only a modest increase was noted for close pore (Supplemental Figure 3).

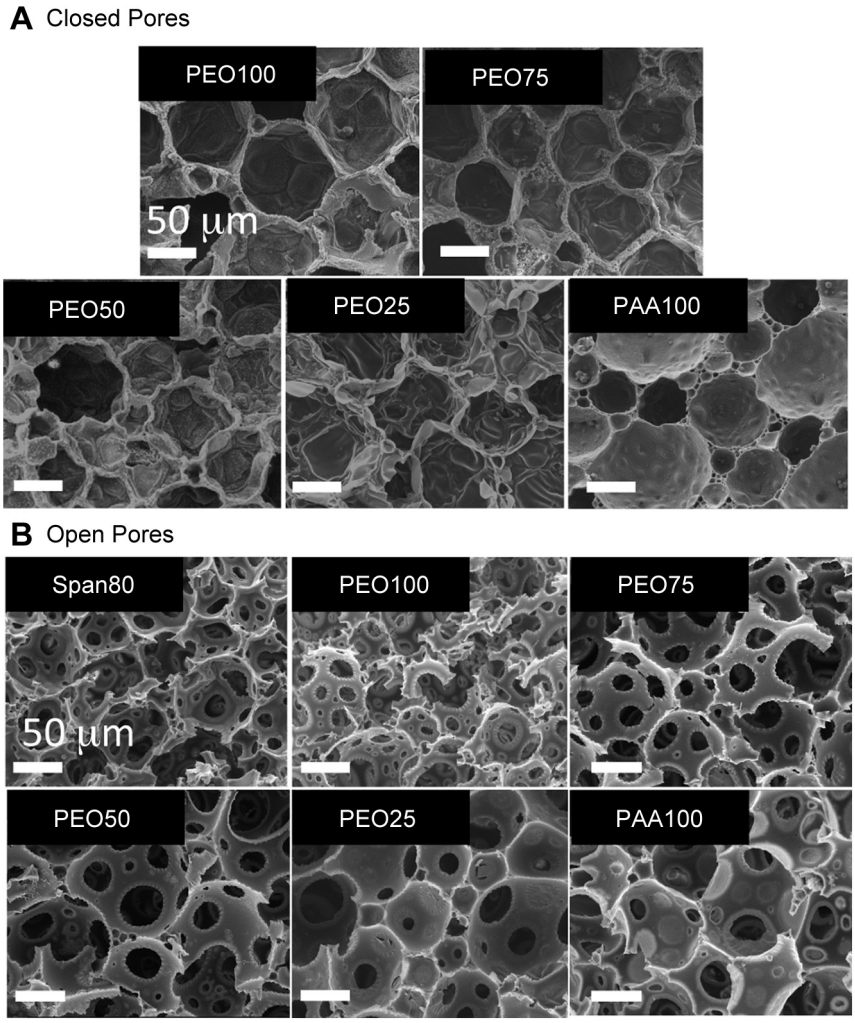

Fig. 1. 3D scaffold morphologies. Scanning electron micrographs of polyHIPE foams with (A) closed pore morphology and (B) interconnected open pore morphology for the indicated copolymer mixtures. Scale bars are 50 μm.

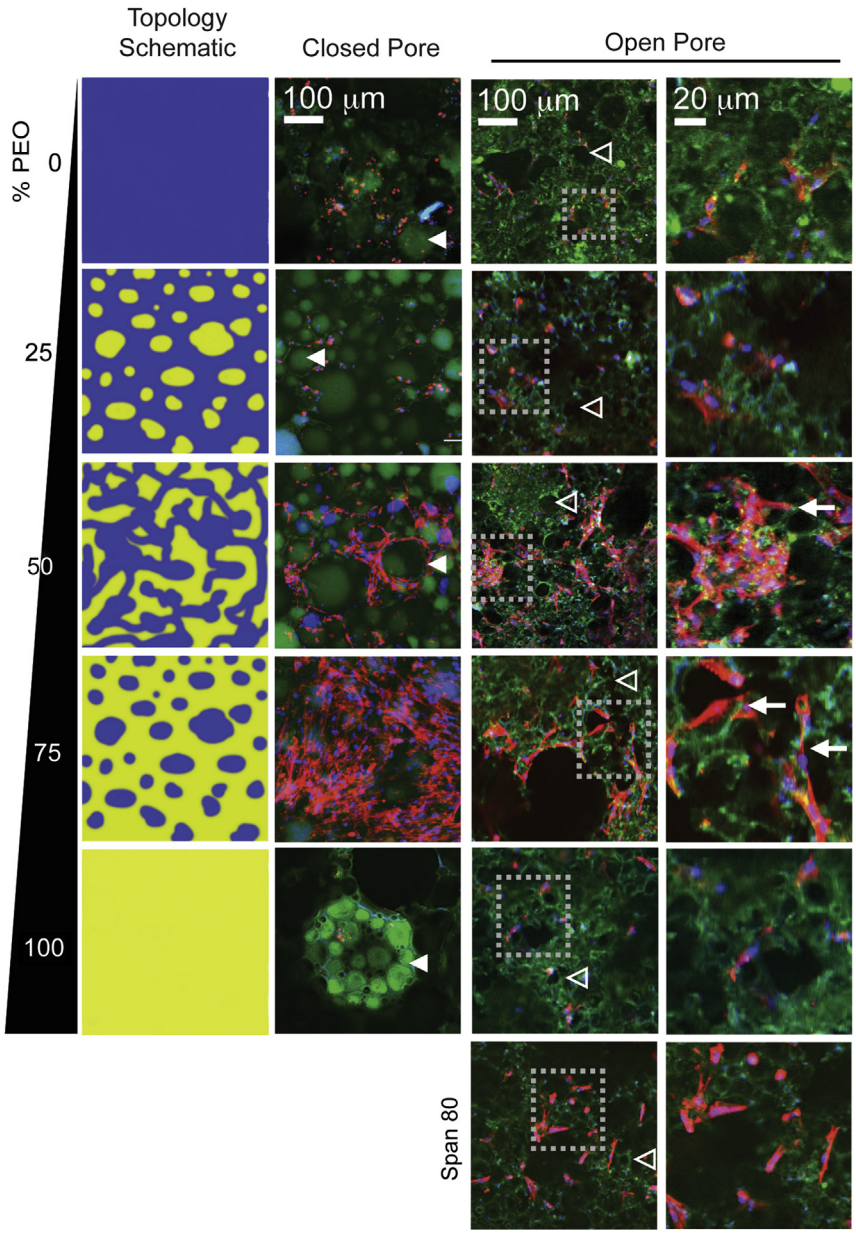

Fig. 2. Differential cell adhesion on polyHIPEs. At the far left is a schematic of the surface topology on the pore walls of polyHIPE foams as a function of PEO molar ratio. Confocal images of filamentous actin (red) and nucleus (blue) staining of hES-MPs cultured on the foams (auto-fluorescence in green) for 7 days show differential adhesion and cell spreading on copolymer functionalized closed porous and open porous foams compared to Span 80 functionalized foams. Solid arrowheads indicate hES-MPs adhering and spreading around the pore struts of the closed porous foams. Open arrowheads indicate hES-MP spreading through the interconnected pores. Dashed lines indicate regions magnified in other images. (For interpretation of the references to color in this figure legend, the reader is referred to the web version of this article.)

Irrespective of foam morphology and the initial amount of cell adhesion, hES-MPs proliferated and spread poorly on foams composed of PEO100 (Fig. 2, bottom), which is consistent with PEO inhibiting protein and cell attachment [31]. Poor cell spreading was also noted for uniformly adhesive PAA100 foams (Fig. 2, top), which is consistent with observations of reduced cell motility and proliferation on substrates with high ligand density [32,33]. In contrast hES-MP adhesion and spreading was the greatest on PEO75 and PEO50 open porous foams (Fig. 2, middle) corroborating the total cell number observed on these compositions by day 7 (Supplemental Figure 2A). Cells cultured on closed porous foams adhered to and spread on either the curved void surface or around the struts of the voids (solid arrows, Fig. 2) whereas cells cultured on open porous foams adhered and spread through the interconnects in a three-dimensional matrix (open arrows, Fig. 2). Since hES-MP cell adhesion and spreading was dependent on scaffold surface topology for open porous foams as it was on closed porous foams, these data imply a similar mechanism with the presence of adhesive nano-domains as was observed with closed porous foams [21].

Beyond 7 days, adhesion and spreading of hES-MPs on open and closed porous foams was also evaluated after 14, 21 and 28 days. Closed porous foams did not support cell proliferation at these time points. However hES-MP cells cultured on open porous foams exhibited cell proliferation across all the copolymer compositions at the specified time points (Supplemental Figure 4). This indicates that although differential cell adhesion occurred in the first week of culture, cells that were initially adherent but not well spread were still able to proliferate over long periods in culture.

Although the surface topology of adhesive domains regulated basic cell functions over 7 days in culture, it was not clear to what extent it would influence hES-MP differentiation over the same time course and beyond. Gene expression for different mesenchymal lineages (Supplemental Table 1) was measured by microarray of hES-MP cells cultured on PEO100, PEO75, PEO50, PEO25, and PAA100 open and closed porous scaffolds normalized to undifferentiated cells (Fig. 3A, B; Supplemental Table 2). While closed pore scaffolds generally exhibited larger changes of individual gene expression than open pore scaffolds, the average fold change for certain lineages was dependent on the scaffold's adhesive surface topology and pore morphology (Fig. 3C); for closed porous foams, mRNA was up-regulated in hES-MP cells in a topology-dependent manner only for mRNA associated with osteogenesis. For open porous foams, osteogenesis was also topology-dependent but osteogenic genes increased with the PEO concentration, unlike closed porous foams. Correlation coefficients to directly compare gene expression between closed and open porous foams across all topologies was strongest for osteogenesis at −0.84, indicating opposing osteogenic gene regulation as a result of foam composition and surface topology.

To validate short-term gene expression, longer-term mineral deposition was assessed after 28 days of culture for open porous foams where cell confluence was independent of surface chemistry at that time point (Supplemental Figure 4); closed porous foams, lacking interconnectivity, inhibited cell viability over the same time course, and thus only cells cultured on open porous scaffolds were examined for mineralization. Cells treated with dexamethasone, a glucocorticoid which stimulates osteogenic differentiation and mineralization [34], deposited more calcium for all scaffold compositions. However without dexamethasone, cells on PEO50 and PEO75 open porous foams deposited the most calcium as measured by alizarin red absorbance (Fig. 4), indicating that copolymer composition and thus the surface topology of adhesive domains alone has the potential to support hES-MP cell differentiation. SEM images showed that cells became confluent on each scaffold (Fig. 5A), but hES-MP cells cultured on PEO75 and PEO50 scaffolds also secreted collagen within scaffold pores (Fig. 5B). High magnification images also showed mineral deposits on these foam compositions (Fig. 5A, arrows), again suggesting preferential osteogenic differentiation on scaffolds that display appropriate surface topology. In the presence of dexamethasone, mineralized layers were present on all surfaces regardless of surface chemical composition (Fig. 5C).

Surface topology of adhesive domains may be most biomimetic on PEO75 foams [21] and the open porous structure then may

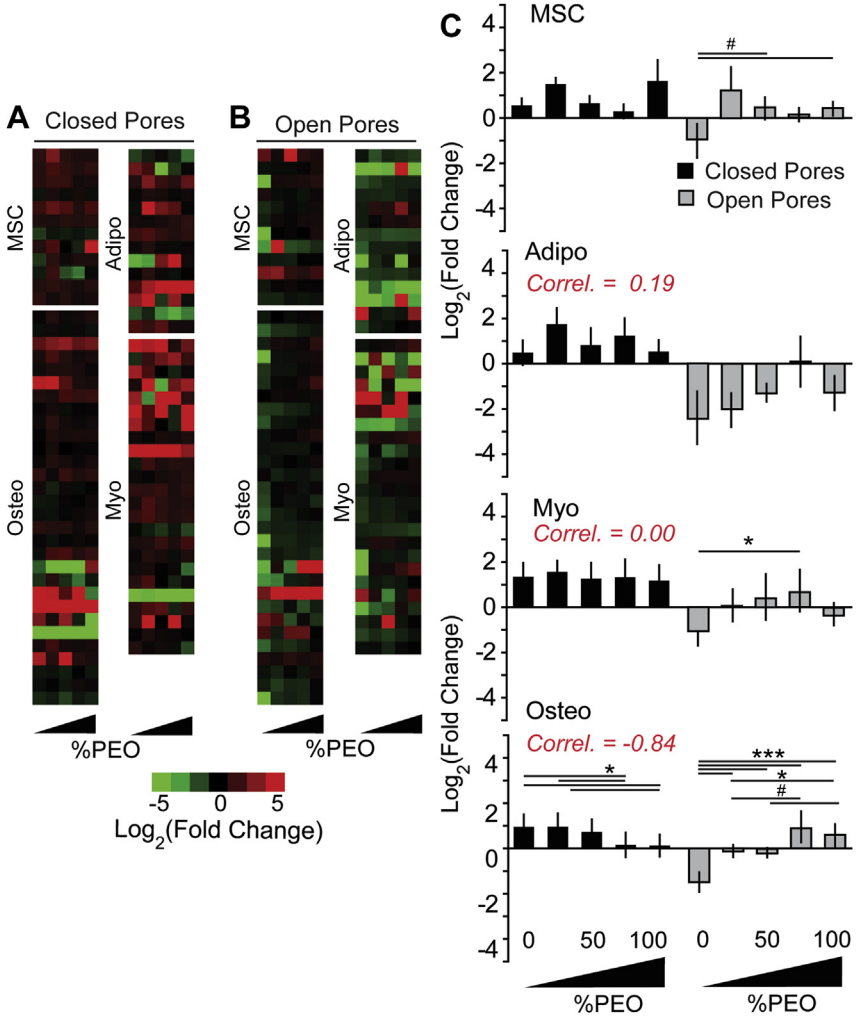

Fig. 3. Lineage specific gene expression. Lineage specific gene expression data as a function of foam PEO% represented as (A) heat maps comparing fold difference change of open and closed porous foams (B) mean fold change comparing open and closed porous foams. The correlation coefficient between the fold change of open and closed porous foams as a function of PEO% is noted. Data is mean ± SEM, n = 3. (C)Mean fold change of lineage specific genes comparing open and closed porous foams. The correlation coefficient between the fold change of open and closed porous foams as a function of PEO% is noted. Data is mean ± SEM, n = 3.

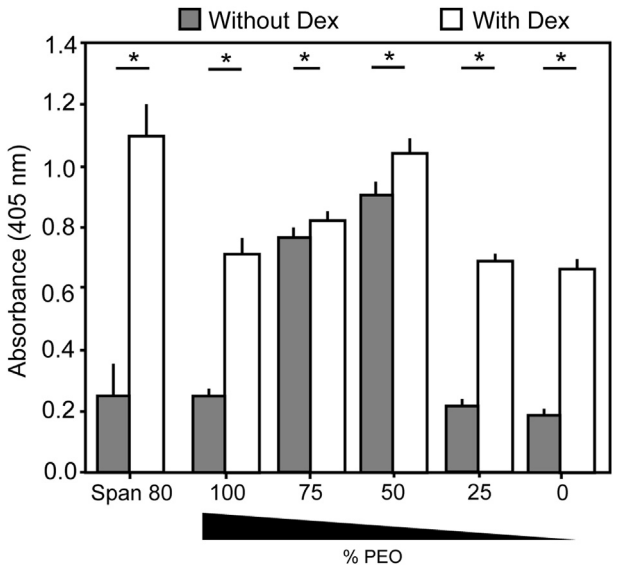

Fig. 4. hES-MP calcium deposition. Calcium deposition assayed by Alizarin Red S. Relative absorbance at 405 for cells treated with and without Dex. n = 9. Significant differences indicated by *p < 0.05.

induce the most robust osteogenic response, but it is still not clear what signaling proteins regulate cell adhesion, spreading, and differentiation on the different surface chemistry and porous structures. Osteogenic gene expression (Supplemental Table 2) was assessed for its correlation with the mean expression of selected cell-matrix signaling genes for both open and closed porous scaffolds (Fig. 6A). Open porous scaffolds exhibited a higher correlation coefficient between average cell-matrix signaling gene expression and osteogenic gene expression. Direct comparisons by two-way ANOVA also confirm these trends, and so to identify specific signaling genes responsible for surface topology-induced osteogenesis, specific signaling gene changes were examined for their correlation with average osteogenic gene expression (Fig. 6B). Integrin-ECM interaction related genes, PTK2 (protein tyrosine kinase 2), also referred to as focal adhesion kinase (FAK), CDC42, and ROCK1 all exhibited the highest correlation coefficients implying a contractile role in surface topology-related signaling similar to other ECM cues including stiffness [35], topography [6], and shape [36].

4. Discussion

4.1. hES-MP adhesion to polyHIPE foams is dependent on surface topology rather than on topography

The onset of differentiation is linked to how and what cells adhere within their extracellular matrix. Matrix properties such as stiffness, topography and surface chemistry have been widely implicated in directing lineage specification [3,4]. While the spatial presentation of adhesive sites on 2D substrates regulates differentiation [16], surface topology's role in 3D matrices has been less well investigated. In the present study, emulsion-templated polyHIPE foams provide a platform for exploiting block copolymer phase separation to generate 3D matrices with adhesive heterogeneity that better reflects the extracellular matrix [3]. Fine-tuning of emulsion parameters allowed further control over scaffold architecture, i.e. closed versus open porosity, to make scaffolds more permissive for

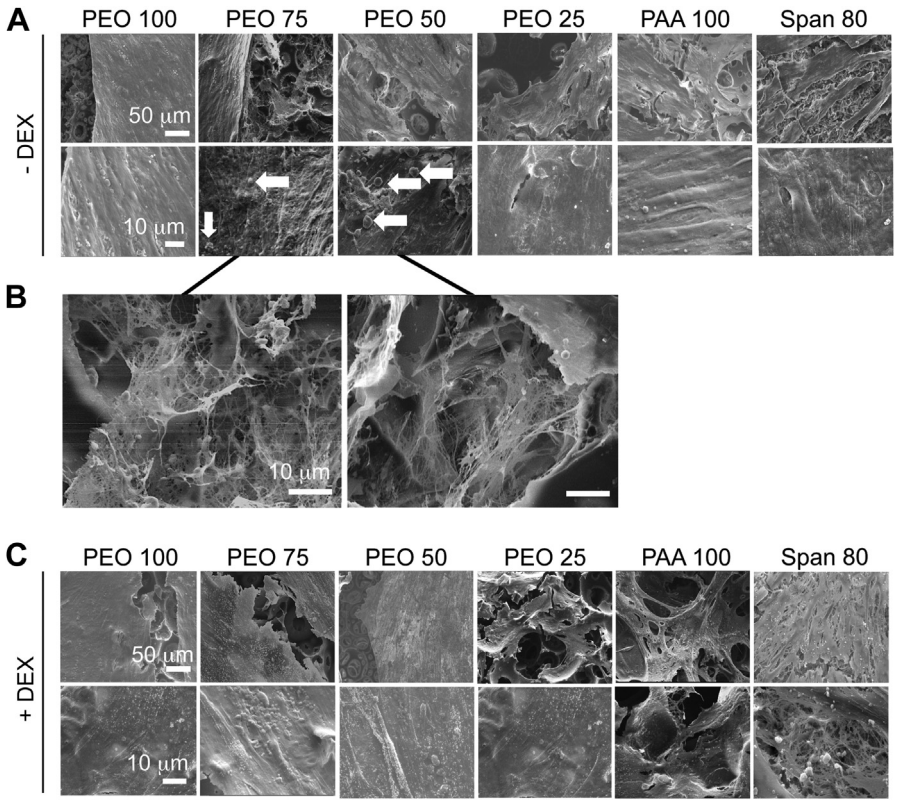

Fig. 5. Matrix and mineral deposition. Representative scanning electron micrographs of hES-MP cells cultured on block copolymer scaffolds for 28 days without DEX (A) and with DEX (C). High magnification images of cells cultured on PEO50 and PEO75 compositions (B) without DEX show cell secreted ECM and mineral deposition indicated by arrowheads and arrows respectively. Arrows indicate mineral nodules.

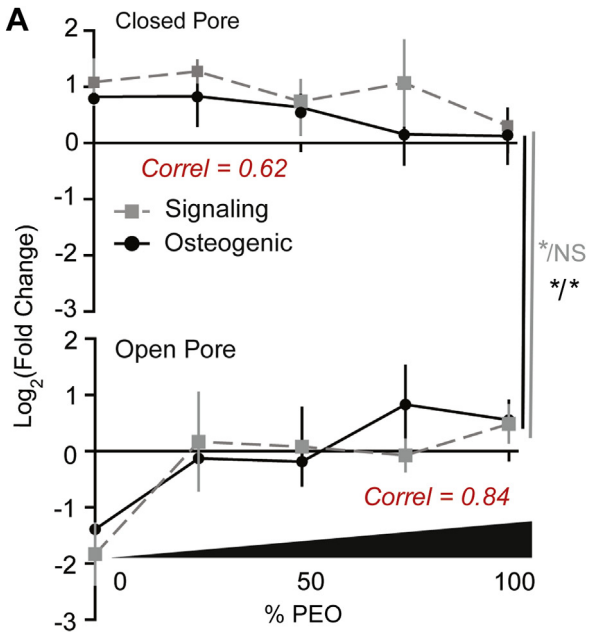

B

	Closed Pore	Open Pore
PTK2	0.890	0.838
RAC1	0.482	0.915
CDC42	0.726	0.786
RHOA	0.687	0.688
ROCK1	0.720	0.869
DIAPH2	0.454	0.838
STARS	-0.045	0.590

Fig. 6. Signaling-osteogenic correlation. (A) Average fold change of signaling and osteogenic genes as a function of foam PEO molar% comparing closed (top) and open (bottom) porous foams. Correlation coefficients between signaling and osteogenic profiles are noted. Data is mean ± SEM. $^{*}p < 0.05$ and N.S. = not significant for two-way ANOVA assessment of significance for foam type (left) and composition (right) variables for signaling (gray) and osteogenic genes (black). (B) Correlation coefficients tabulated between average fold change of osteogenic genes and specific signaling genes (indicated by name) as a function of PEO molar%. A high correlation coefficient indicates influence by a particular signaling gene on osteogenic gene expression.

cell infiltration and longer-term differentiation assays required to assess surface topology's influence over stem cell fate.

As first consideration for these scaffolds, topographical features are well known to regulate stem cell adhesion, cytoskeletal organization [37], signaling [38], and fate between osteogenic or adipogenic lineages [6,39]. In closed porous foams, surface topographical features appear mildly dependent on polymerization conditions, though all compositions have surface roughness below 50 nm [21]. In open porous foams, SEM analysis showed that foams did not exhibit substantially higher surface roughness than closed porous foams (Fig. 1). Previous reports indicate that features in excess of 70 nm promote cell adhesion, likely via integrin clustering [40], and differentiation [6,41]. Thus while foams do not have completely smooth surfaces, they may not have induced osteogenesis. The conditions that caused the roughness in closed porous foams may be associated with the internal phase water droplets having excess surface tension [42]; while this is normally dissipated by coalescence to form interconnecting pores, in this case, the excess surface tension could lead to the formation of finger instabilities at the oil/water interface that create surface topographies. However, the strongest evidence that topographical features were less influential is the observation of composition-dependent and opposing responses for osteogenic genes in hES-MP cells grown in open and closed porous foams (Fig. 3). These data suggest that other HIPE properties, e.g. adhesive domains and pore interconnectivity, could possibly account for differential effects on differentiation, which is discussed below.

4.2. Osteogenic differentiation may be regulated by topology and porosity

Gene expression of hES-MP cells cultured on open and closed porous foams implicated osteogenesis as being dependent on pore morphology, but with a strongly negative correlation coefficient between the two foam structures. While neither program was highly upregulated, subsequent topology-dependent mineralization suggests the importance of the particular osteogenic genes that were highly up-regulated. One such candidate were the BMPs, which have been previously described as regulators of osteogenic differentiation [43,44]. We found that bone morphogenic protein 5 (BMP5) increased for both open and closed pore foams but specifically peaked at PEO75 for open pore foams. Additionally, osteopontin and TWIST-2 were up-regulated on closed pore foams, both peaking at approximately PEO25, suggesting that the porous structure as well as the composition dependent adhesive topology influences osteogenesis. TWIST-2 is known to be a critical early regulator for osteogenic differentiation by inhibition of RUNX2 [45], while osteopontin has shown to interact with specific integrins, which is important for osteogenic differentiation in mesenchymal stem cells.[47] These results imply that the porous structure in addition to the topology may influence osteogenic differentiation as cells can better attach and spread over a larger volume and appear more 3D than in closed porous foams where cells may likely feel a more 2D.

Human Mesenchymal Stem Cell (hMSC) differentiation ultimately depends on stiffness-mediated, Rho-ROCK-induced contractility [35,36,46] and would therefore expect stiff polystyrene scaffolds used here to support osteogenesis independent of surface topology. However, cell contractility depends on sufficient cell adhesion to pull against the underlying matrix [36]. Furthermore adhesion mediated activation of focal adhesion kinase (FAK) has been shown to be important in early commitment of ostegenic differentiation of hMSCs [47]. FAK activation has been implicated in triggering extracellular regulating kinase 1/2 (ERK1/2) signaling to induce osteogenesis of mesenchymal stem cells [48]. Yee et al. have hypothesized that increased adhesion via $\alpha 5\beta 1$ integrins activated ERK1/2 signaling via FAK [49]. Taken together, our data suggest that differentiation is not just linked to stiffness-induced changes in cell morphology but rather to stiffness regulated integrin signaling and adhesive organization, much like occur in other 3D systems [50]. The wider implication of our data in the context of biomaterial design is that complex differentiation pathways may be triggered via structural organization of early adhesion events, i.e. adhesive heterogeneity.

5. Conclusions

We have demonstrated the use of emulsion templated foams containing heterogeneously spaced adhesive nano-domains in guiding mesenchymal stem cell adhesion and differentiation. Adhesive patches that better reflect the adhesive spacing found in ECM allowed for the greatest amount of cell spreading irrespective of scaffold architecture. Introducing porosity by varying polyHIPE polymerization parameters increased the likelihood of

osteospecific differentiation in a topology dependent manner. In this study we use stiff polystyrene matrices; modifying stiffness by altering matrix chemistry independently of scaffold topology could further fine-tune the scaffold's properties to allow differentiation of mesenchymal stem cells towards other lineages.

Acknowledgments

The authors would like to thank the Electron Microscopy Unit and the Light Microscopy Unit at The University of Sheffield for use of their facilities. The authors acknowledge funding from the Human Frontier Science Program (RGY0064/2010 to A.J.E. and G.B.), the National Institutes of Health (DP02OD006460 to A.J.E.), the National Science Foundation Graduate Research Fellowship Program (to M.O.), and the Royal Thai Government Science and Technology Pre-doctoral Fellowship program (to S.C.).

Appendix A. Supplementary data

Supplementary data related to this article can be found at http://dx.doi.org/10.1016/j.biomaterials.2015.01.034.

References

[1] Geiger B, Bershadsky A, Pankov R, Yamada KM. Transmembrane crosstalk between the extracellular matrix–cytoskeleton crosstalk. Nat Rev Mol Cell Biol 2001;2:793–805.
[2] Huang S, Ingber DE. The structural and mechanical complexity of cell-growth control. Nat Cell Biol 1999;1:E131–8.
[3] Reilly GC, Engler AJ. Intrinsic extracellular matrix properties regulate stem cell differentiation. J Biomech 2010;43:55–62.
[4] Discher DE, Mooney DJ, Zandstra PW. Growth factors, matrices, and forces combine and control stem cells. Science 2009;324:1673–7.
[5] Vogel V, Sheetz M. Local force and geometry sensing regulate cell functions. Nat Rev Mol Cell Biol 2006;7:265–75.
[6] Dalby MJ, Gadegaard N, Tare R, Andar A, Riehle MO, Herzyk P, et al. The control of human mesenchymal cell differentiation using nanoscale symmetry and disorder. Nat Mater 2007;6:997–1003.
[7] Guilak F, Cohen DM, Estes BT, Gimble JM, Liedtke W, Chen CS. Control of stem cell fate by physical interactions with the extracellular matrix. Cell Stem Cell 2009;5:17–26.
[8] Ayala R, Zhang C, Yang D, Hwang Y, Aung A, Shroff SS, et al. Engineering the cell-material interface for controlling stem cell adhesion, migration, and differentiation. Biomaterials 2011;32:3700–11.
[9] Flaim CJ, Chien S, Bhatia SN. An extracellular matrix microarray for probing cellular differentiation. Nat Methods 2005;2:119–25.
[10] Young JL, Engler AJ. Hydrogels with time-dependent material properties enhance cardiomyocyte differentiation in vitro. Biomaterials 2011;32:1002–9.
[11] DeForest CA, Anseth KS. Cytocompatible click-based hydrogels with dynamically tunable properties through orthogonal photoconjugation and photocleavage reactions. Nat Chem 2011;3:925–31.
[12] Jeon O, Alsberg E. Photofunctionalization of alginate hydrogels to promote adhesion and proliferation of human mesenchymal stem cells. Tissue Eng Part A 2013;19:1424–32.
[13] Khetan S, Burdick JA. Patterning network structure to spatially control cellular remodeling and stem cell fate within 3-dimensional hydrogels. Biomaterials 2010;31:8228–34.
[14] Luo W, Chan EW, Yousaf MN. Tailored electroactive and quantitative ligand density microarrays applied to stem cell differentiation. J Am Chem Soc 2010;132:2614–21.
[15] Luo W, Yousaf MN. Tissue morphing control on dynamic gradient surfaces. J Am Chem Soc 2011;133:10780–3.
[16] Frith JE, Mills RJ, Cooper-White JJ. Lateral spacing of adhesion peptides influences human mesenchymal stem cell behaviour. J Cell Sci 2012;125:317–27.
[17] Mao Y, Schwarzbauer JE. Fibronectin fibrillogenesis, a cell-mediated matrix assembly process. Matrix Biol 2005;24:389–99.
[18] Vogel V. Mechanotransduction involving multimodular proteins: converting force into biochemical signals. Annu Rev Biophys Biomol Struct 2006;35:459–88.
[19] Huang J, Grater SV, Corbellini F, Rinck S, Bock E, Kemkemer R, et al. Impact of order and disorder in RGD nanopatterns on cell adhesion. Nano Lett 2009;9:1111–6.
[20] Altrock E, Muth CA, Klein G, Spatz JP, Lee-Thedieck C. The significance of integrin ligand nanopatterning on lipid raft clustering in hematopoietic stem cells. Biomaterials 2012;33:3107–18.
[21] Viswanathan P, Chirasatitsin S, Ngamkham K, Engler AJ, Battaglia G. Cell instructive microporous scaffolds through interface engineering. J Am Chem Soc 2012;134:20103–9.
[22] George PA, Quinn K, Cooper-White JJ. Hierarchical scaffolds via combined macro- and micro-phase separation. Biomaterials 2010;31:641–7.
[23] LoPresti C, Massignani M, Fernyhough C, Blanazs A, Ryan AJ, Madsen J, et al. Controlling polymersome surface topology at the nanoscale by membrane confined polymer/polymer phase separation. ACS Nano 2011;5:1775–84.
[24] Massignani M, LoPresti C, Blanazs A, Madsen J, Armes SP, Lewis AL, et al. Controlling cellular uptake by surface chemistry, size, and surface topology at the nanoscale. Small 2009;5:2424–32.
[25] Gurevitch I, Silverstein MS. Polymerized pickering HIPEs: effects of synthesis parameters on porous structure. J Polym Sci Polym Chem 2010;48:1516–25.
[26] Robinson JL, Moglia RS, Stuebben MC, McEnery MA, Cosgriff-Hernandez E. Achieving interconnected pore architecture in injectable polyHIPEs for bone tissue engineering. Tissue Eng Part A 2014;20:1103–12.
[27] Bokhari M, Carnachan RJ, Przyborski SA, Cameron NR. Emulsion-templated porous polymers as scaffolds for three dimensional cell culture: effect of synthesis parameters on scaffold formation and homogeneity. J Mater Chem 2007;17:4088–94.
[28] Karlsson C, Emanuelsson K, Wessberg F, Kajic K, Axell MZ, Eriksson PS, et al. Human embryonic stem cell-derived mesenchymal progenitors–potential in regenerative medicine. Stem Cell Res 2009;3:39–50.
[29] Delaine-Smith RM, MacNeil S, Reilly GC. Matrix production and collagen structure are enhanced in two types of osteogenic progenitor cells by a simple fluid shear stress stimulus. Eur Cell Mater 2012;24:162–74.
[30] Schmittgen TD, Livak KJ. Analyzing real-time PCR data by the comparative C(T) method. Nat Protoc 2008;3:1101–8.
[31] Hoffman AS. Non-fouling surface technologies. J Biomater Sci Polym Ed 1999;10:1011–4.
[32] Maheshwari G, Brown G, Lauffenburger DA, Wells A, Griffith LG. Cell adhesion and motility depend on nanoscale RGD clustering. J Cell Sci 2000;113(Pt 10):1677–86.
[33] Gallant ND, Michael KE, Garcia AJ. Cell adhesion strengthening: contributions of adhesive area, integrin binding, and focal adhesion assembly. Mol Biol Cell 2005;16:4329–40.
[34] Pitaru S, Kotev-Emeth S, Noff D, Kaffuler S, Savion N. Effect of basic fibroblast growth factor on the growth and differentiation of adult stromal bone marrow cells: enhanced development of mineralized bone-like tissue in culture. J Bone Min Res 1993;8:919–29.
[35] Engler AJ, Sen S, Sweeney HL, Discher DE. Matrix elasticity directs stem cell lineage specification. Cell 2006;126:677–89.
[36] McBeath R, Pirone DM, Nelson CM, Bhadriraju K, Chen CS. Cell shape, cytoskeletal tension, and RhoA regulate stem cell lineage commitment. Dev Cell 2004;6:483–95.
[37] Yim EK, Darling EM, Kulangara K, Guilak F, Leong KW. Nanotopography-induced changes in focal adhesions, cytoskeletal organization, and mechanical properties of human mesenchymal stem cells. Biomaterials 2010;31:1299–306.
[38] Seo CH, Furukawa K, Montagne K, Jeong H, Ushida T. The effect of substrate microtopography on focal adhesion maturation and actin organization via the RhoA/ROCK pathway. Biomaterials 2011;32:9568–75.
[39] Wang PY, Li WT, Yu J, Tsai WB. Modulation of osteogenic, adipogenic and myogenic differentiation of mesenchymal stem cells by submicron grooved topography. J Mater Sci Mater Med 2012;23:3015–28.
[40] Geblinger D, Addadi L, Geiger B. Nano-topography sensing by osteoclasts. J Cell Sci 2010;123:1503–10.
[41] Oh S, Brammer KS, Li YS, Teng D, Engler AJ, Chien S, et al. Stem cell fate dictated solely by altered nanotube dimension. Proc Natl Acad Sci U S A 2009;106:2130–5.
[42] Williams JM. High internal phase water-in-oil emulsions – influence of surfactants and cosurfactants on emulsion stability and foam quality. Langmuir 1991;7:1370–7.
[43] Li M, Li X, Meikle MC, Islam I, Cao T. Short periods of cyclic mechanical strain enhance triple-supplement directed osteogenesis and bone nodule formation by human embryonic stem cells in vitro. Tissue Eng Part A 2013;19:2130–7.
[44] Haque T, Hamade F, Alam N, Kotsiopriftis M, Lauzier D, St-Arnaud R, et al. Characterizing the BMP pathway in a wild type mouse model of distraction osteogenesis. Bone 2008;42:1144–53.
[45] Bialek P, Kern B, Yang X, Schrock M, Sosic D, Hong N, et al. A twist code determines the onset of osteoblast differentiation. Dev Cell 2004;6:423–35.
[46] Kilian KA, Bugarija B, Lahn BT, Mrksich M. Geometric cues for directing the differentiation of mesenchymal stem cells. Proc Natl Acad Sci U S A 2010;107:4872–7.
[47] Shih YR, Tseng KF, Lai HY, Lin CH, Lee OK. Matrix stiffness regulation of integrin-mediated mechanotransduction during osteogenic differentiation of human mesenchymal stem cells. J Bone Min Res 2010;26:730–8.
[48] Salasznyk RM, Klees RF, Williams WA, Boskey A, Plopper GE. Focal adhesion kinase signaling pathways regulate the osteogenic differentiation of human mesenchymal stem cells. Exp Cell Res 2007;313:22–37.
[49] Yee KL, Weaver VM, Hammer DA. Integrin-mediated signalling through the MAP-kinase pathway. IET Syst Biol 2008;2:8–15.
[50] Huebsch N, Arany PR, Mao AS, Shvartsman D, Ali OA, Bencherif SA, et al. Harnessing traction-mediated manipulation of the cell/matrix interface to control stem-cell fate. Nat Mater 2010;9:518–26.